EarthArXiv Coversheet

Uncertainty-Aware Bayesian Machine Learning for Landslide Susceptibility Mapping: in the Chattogram Metropolitan Hill System, Bangladesh

Authors and Affiliations

Golam Murad

Graduate, Department of Civil Engineering, Chittagong University of Engineering & Technology, Chattogram-4349, Bangladesh

Email: u1901087@student.cuet.ac.bd

Shotabdy Chowdhury Srabony

Research Assistant, Department of Civil Engineering, Chittagong University of Engineering & Technology, Chattogram-4349, Bangladesh

Email: u1901052@student.cuet.ac.bd

Shafiq Mahmud

Undergraduate Student, Department of Urban and Regional Planning, Chittagong University of Engineering & Technology, Chattogram-4349, Bangladesh

Email: u2105051@student.cuet.ac.bd

Md. Aftabur Rahman*

Professor, Department of Civil Engineering, Chittagong University of Engineering & Technology, Chattogram-4349, Bangladesh

Email: maftabur@cuet.ac.bd

Corresponding author: Md. Aftabur Rahman

Correspondence email: maftabur@cuet.ac.bd

Uncertainty-Aware Bayesian Machine Learning for Landslide Susceptibility Mapping: in the Chattogram Metropolitan Hill System, Bangladesh

Golam Murad[1], Shotabdy Chowdhury Srabony[2], Shafiq Mahmud[2], Md. Aftabur Rahman[3*]

[1]Graduate, Department of Civil Engineering, Chittagong University of Engineering & Technology, Chattogram-4349, Bangladesh, Email: u1901087@student.cuet.ac.bd

[2]Research Assistant, Department of Civil Engineering, Chittagong University of Engineering & Technology, Chattogram-4349, Bangladesh, Email: u1901052@student.cuet.ac.bd

[2]Undergraduate Student, Department of Urban and Regional Planning, Chittagong University of Engineering & Technology, Chattogram-4349, Bangladesh, Email: u2105051@student.cuet.ac.bd

[3]Professor, Department of Civil Engineering, Chittagong University of Engineering & Technology, Chattogram-4349, Bangladesh, Email: maftabur@cuet.ac.bd

*Corresponding Author: Md. Aftabur Rahman

Abstract

Landslide-prone hilly regions experiencing rapid urban expansion need susceptibility models that provide both robust predictive performance and transparent uncertainty estimates. This study develops an uncertainty-aware probabilistic framework for landslide susceptibility mapping in Bangladesh's Chattogram metropolitan hill system, incorporating 14 conditioning factors: geomorphological, hydrological, environmental, and anthropogenic. Multicollinearity analysis, i.e., VIF and tolerance, verified the statistical stability of the predictors. We compared four classifiers, Bayesian Logistic Regression, Gaussian Process Classifier, L2-regularized Logistic Regression, and Random Forest, within a standardized preprocessing pipeline. Models were evaluated using cross-validation, holdout testing, and spatial block validation, with metrics for discrimination, robustness, and calibration. Random Forest had the strongest discrimination (ROC-AUC = 0.866; MCC = 0.611) on the holdout set, while the Gaussian Process Classifier showed better probability calibration (ECE = 0.084) with competitive discrimination (ROC-AUC = 0.821) among Bayesian models. Susceptibility and uncertainty were combined in a 3×3 scheme to visualize hazard and confidence. Mapping showed that 78.71% of landslides were in the Very High class, covering only 9.47% of the area (SCAI = 0.12). These results show that uncertainty-aware Bayesian modeling with bivariate spatial integration enhances interpretability and provides transparent hazard assessments in data-limited urban hill areas.

Keywords: Landslide susceptibility; Bayesian inference; Gaussian processes; Uncertainty quantification; SCAI.

Introduction

Landslides are complex geohazards that result from interactions among geological, lithological, hydrological, and human factors (Roy et al., 2025). They cause significant loss of human life and damage to infrastructure in mountains and hilly areas worldwide (Tsompanakis et al., 2023). Due to rapid land-use change and heavy rainfall, their impact is becoming more significant (Ehsan et al., 2025). Landslides are among the most frequent lithosphere hazards, and their occurrence in Bangladesh has been increasing for the last 20 years (Hafsa et al., 2022). Therefore, spatially explicit landslide susceptibility maps (LSMs) serve as targeted tools for land use planning, early warning systems, and disaster risk reduction (Chowdhury et al., 2023).

The predictive ability of LSMs has been greatly enhanced by recent developments in remote sensing, geographic information systems (GIS), and machine learning (Poddar & Roy, 2026). However, there are still two methodological challenges. First, despite having high predictive accuracy, models often fail to generalize spatially, especially when evaluation relies on naïve random cross-validation that does not account for spatial autocorrelation (Adnan et al., 2020; Koldasbayeva et al., 2024). Second, many models provide only deterministic point predictions without uncertainty estimates, which makes them less useful for decision-making under risk (Milà et al., 2024).

Common machine learning algorithms like Random Forest and Support Vector Machines tend to maximize classification accuracy. However, they do not, by default, offer well-calibrated probabilistic outputs or explicit uncertainty quantification (Shaker & Hüllermeier, 2025). As a result, predictions may appear overconfident when transferred to novel terrain conditions. On the other hand, the Bayesian approach treats model parameters as probability distributions instead of fixed numbers. This allows for the formal propagation of epistemic uncertainty into posterior predictive distributions (Mirus & Woodard, 2023). Such models are well-suited for risk management, as they not only yield high predicted risks but also explicit statements of the confidence in those predictions (Stefanini et al., 2025).

In Bangladesh, Chittagong Hill Tracts and metropolitan areas represent a setting where improved LSM practices are urgently needed. This region is highly susceptible to landslides for several reasons, such as steep slopes, intense monsoon rainfall, and escalating human encroachment (Biswas et al., 2026). During the monsoon, the frequency of landslides becomes a significant threat in this area, which eventually causes fatalities and socio-economic losses (Roy et al., 2025). Traditional GIS methods, logistic regression, decision tree variants, ensemble tree-based models and some deep learning models have shown strong performance in discriminating landslide susceptibility in regional susceptibility studies (Roy et al., 2025). However, a considerable number of these studies lack proper spatial data resolution, lack spatial validation and sufficient uncertainty quantification. Addressing these shortcomings is essential for effective disaster risk reduction in such a dynamic environment (Rahman et al., 2025).

Recent research efforts on data-driven LSMs have evolved towards two main pathways. The former focuses on optimizing algorithmic performance metrics, such as the area under the receiver operating characteristic curve (AUC) and accuracy when using ensemble strategies, while the latter combines evaluation data with generation data (Zhou & Xing, 2025). The hybrid and stacked models usually perform better than single learners. These models are also fairly complex, making them less explainable (SINDHU, 2025). The second direction, which emphasizes a methodological domain in its evaluation for LSMs (spatial validation, probabilistic calibration and uncertainty quantification) as essential elements of any robust model (C. H. Cheng & Fan, 2024).

Bayesian machine learning addresses these limitations in a coherent manner. Bayesian logistic regression and Gaussian process classifiers are machine learning algorithms that provide posterior predictions instead of point estimate (W.-J. Yan et al., 2025). This ability is especially advantageous in hilly urban settings, where significant epistemic uncertainty accompanies landslide susceptibility across data-poor contexts because of diverse and overlapping conditioning factors (Chowdhury et al., 2023). In addition, mitigation actions such as the reinforcement of slopes, improvement of drainage, or even relocation need to be informed not only by where landslides are likely to happen but also by how confident we are in these predictions (Pareek et al., 2024).

Addressing these methodological and practical gaps, this study proposes a reproducible and uncertainty-aware modeling framework for LSM at urban hillslopes in regions like Chittagong, Bangladesh. The framework incorporates spatial validation, probabilistic calibration assessment, and uncertainty quantification. We compare performance estimates (statistically robust and spatially realistic) under repeated stratified cross-validation, spatial block cross-validation, and independent holdout testing for both deterministic and Bayesian classifiers. Model evaluation goes beyond measures of discrimination, but also includes calibration metrics that assess how predicted probabilities relate to observed rates of landslide occurrence. Although several algorithms are benchmarked under identical conditions, final deployment is limited to Bayesian classifiers that generate posterior predictive distributions and associated uncertainty surfaces.

This study contributes to improving LSM practice for evidence-based intervention planning in data-scarce urban hill regions through the integration of predictive accuracy, strong spatial validation, probabilistic classification, and explicit uncertainty representation.

Study Area and Data

Study area

The study area is situated in the Chattogram Metropolitan Area (CMA), Bangladesh. CMA is located roughly between (22°06′N–22°34′N) latitude and (91°40′E–92°02′E) longitude, covering an area of about 775 km² (Chowdhury et al., 2023). Within CMA, the study area covers a spatially continuous terrain covering Fatehpur Union and parts of several wards under Chattogram City Corporation (CCC) jurisdiction, as well as adjacent administrative areas associated with Bayezid Bostami, Khulshi, Kotwali, and Panchlaish thanas (Ahmed, 2014).

The studied region is characterized by a typical geomorphological feature of Chattogram metropolitan hill system, an amalgamated topography composed of varied elevations, moderate to steep slopes separated from each other by low-lying plains (Islam et al., 2021). Elevation can change significantly over short spatial distances, leading to localized areas of slope instability (Song et al., 2023). Natural relief has been modified due to rapid urban growth, hill cutting, road construction, and changing land use, which has increased landslide susceptibility (Hen-Jones et al., 2025).

Regarding climatic conditions, the region falls in a tropical monsoon zone with high seasonal rainfall during the monsoon period (June–September) (Rahman et al., 2025). Heavy continuous rain increases soil moisture, decreases shear strength and raise the risk of landslide (Hamza et al., 2025). The area studied was selected due to the documented occurrence of landslides combined with heterogeneous terrain, an area subject to urban infrastructure and building construction development pressures. These attributes render it an ideal case for probabilistic landslide-susceptibility modeling and subsequent infrastructure-vulnerability assessment, employing geospatial and Bayesian machine-learning techniques.

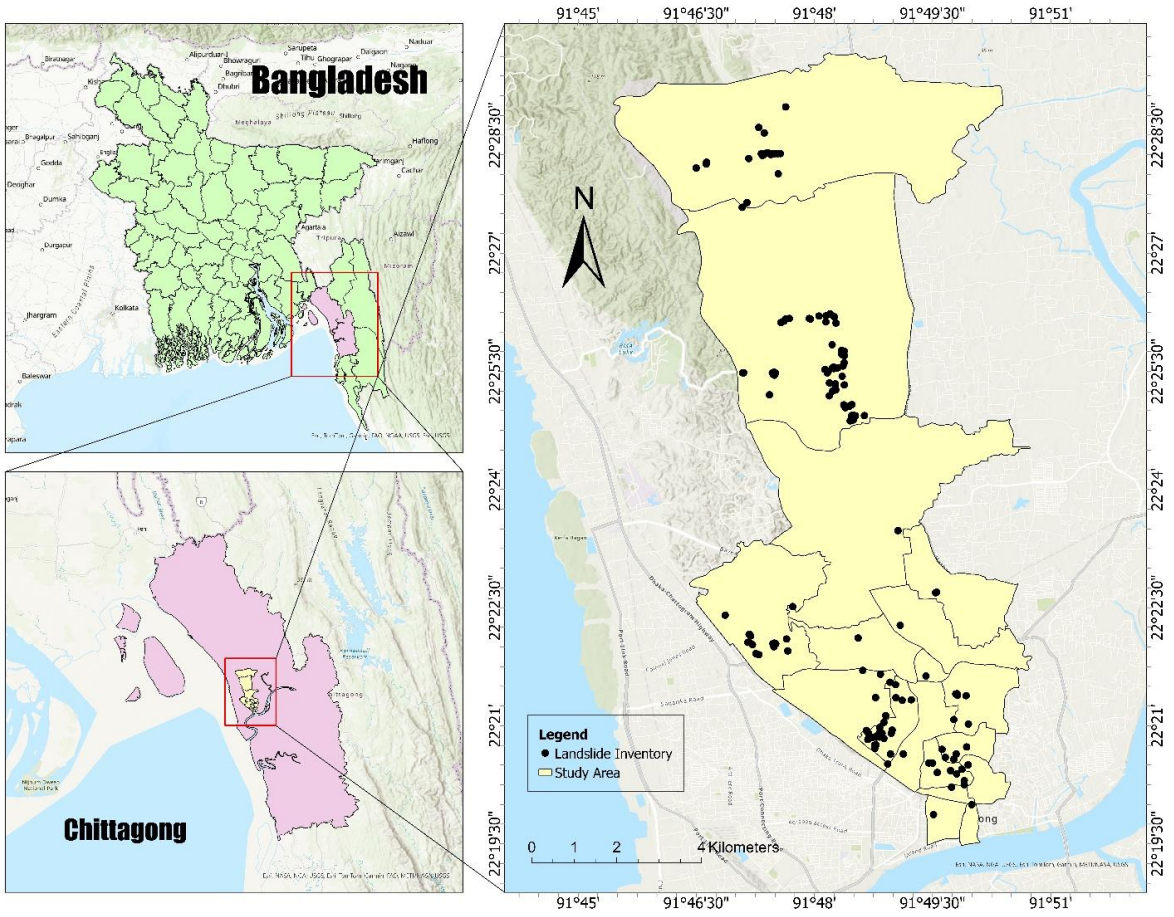

Figure 1: Study Area with Landslide Inventory Points

Landslide inventory

The landslide inventory map is the primary step of this research. The historical landslide locations were collected from several credible datasets such as NASA's global landslide catalog dataset, the Centre for Environmental and Geographic Information Services (CEGIS), the Bangladesh Army, and some related literature records (Rabby & Li, 2019). Overall, 155 validated landslide points were recognized in our study area, encompassing various topographical and geomorphological conditions. These sites were treated as point features in a GIS environment to create an overall landslide inventory map that can be used for modelling susceptibility. In addition to those recorded at the landslide points, around 200 non-landslide alternatives were randomly synthesized from stable places devoid of any historical landslide incidents (Xia et al., 2023).

Landslide Conditioning Factors

Based on a literature review and availability of data, fourteen conditioning factors representing topographic (slope, aspect, elevation), hydrological (drainage density), environmental (land use land cover), proximity (distance to road, distance to river), and soil-related factors were selected (Table 1). All raster layers were resampled to a consistent 30-m spatial resolution for data analysis (Adnan et al., 2020).

Topographic derivatives, including slope, aspect, curvature, SPI, TWI, and TRI, were extracted from the 30 m SRTM DEM (Sun et al., 2021). Hydrological and proximity-related variables were generated from DEM-based drainage networks and OpenStreetMap road data (Tai et al., 2020). Vegetation and land cover information were derived from Landsat 8 Level-2 surface reflectance imagery (NDVI) and Esri Sentinel-2 Land Cover data (10 m, resampled to 30 m) (Tulbure et al., 2022). Precipitation data were obtained from the CHIRPS dataset (5 km resolution), and soil texture data were sourced from the ISRIC SoilGrids (250 m resolution) (Cunha et al., 2018).

Categorical variables (aspect, LULC, and soil texture) were transformed using one-hot encoding to avoid artificial ordinality in machine learning models (Hengl et al., 2017).

Table 1: Landslide Conditioning Factors

Factor	Source of Data	Spatial Resolution (m)
Elevation	https://earthexplorer.usgs.gov/ SRTM DEM	30 m × 30 m
Slope	https://earthexplorer.usgs.gov/ Derived from SRTM DEM	30 m × 30 m
Aspect	https://earthexplorer.usgs.gov/ Derived from SRTM DEM	30 m × 30 m
Curvature	https://earthexplorer.usgs.gov/ Derived from SRTM DEM	30 m × 30 m
SPI	https://earthexplorer.usgs.gov/ Derived from SRTM DEM	30 m × 30 m
TWI	https://earthexplorer.usgs.gov/ Derived from SRTM DEM	30 m × 30 m
TRI	https://earthexplorer.usgs.gov/ Derived from SRTM DEM	30 m × 30 m
NDVI	https://earthexplorer.usgs.gov/ Landsat 8 Level-2 Surface Reflectance	30 m × 30 m
LULC	https://livingatlas.arcgis.com/landcover/ Esri Sentinel-2 Land Cover	10 m × 10 m
Rainfall	https://www.chc.ucsb.edu/data/chirps CHIRPS Precipitation Dataset	5000 m × 5000 m
Drainage Density	https://earthexplorer.usgs.gov/ Derived from SRTM DEM	30 m × 30 m
Distance to River	https://earthexplorer.usgs.gov/ Derived from drainage network (SRTM DEM)	30 m × 30 m

Distance to Road	https://www.openstreetmap.org/ OpenStreetMap Road Network	30 m × 30 m
Soil Texture	https://soilgrids.org/ ISRIC SoilGrids	250 m × 250 m

The spatial patterns of the fourteen conditioning factors are presented in **Figure 1**.

In our study area, elevation ranges from −0.9 m to 88 m and is classified into five altitudinal intervals. Slope values were grouped into six classes (0–5°, 5–10°, 10–15°, 15–20°, 20–25°, and 25–35°), reflecting gradual to moderately steep terrain conditions. Aspect was categorized into eight cardinal directions.

Curvature values were divided into five classes representing concave to convex terrain forms. SPI and TWI were derived from hydrological analysis of the DEM and categorized into five classes each, representing increasing flow accumulation and soil moisture potential, respectively. TRI was grouped into five classes to represent increasing terrain ruggedness.

The LULC layer was classified into seven categories: water bodies, trees, flooded vegetation, cropland, built-up areas, barren land, and rangeland. NDVI values were reclassified into five vegetation-density levels.

Mean annual precipitation ranges between approximately 2,983 mm and 3,150 mm and was grouped into seven intensity classes. Drainage density was categorized into seven classes reflecting increasing channel concentration. Euclidean distances to rivers and roads were classified into seven proximity intervals to represent the influence of fluvial erosion and the intensity of anthropogenic disturbance. Soil texture was categorized into three dominant classes: sandy loam, loam, and clay loam.

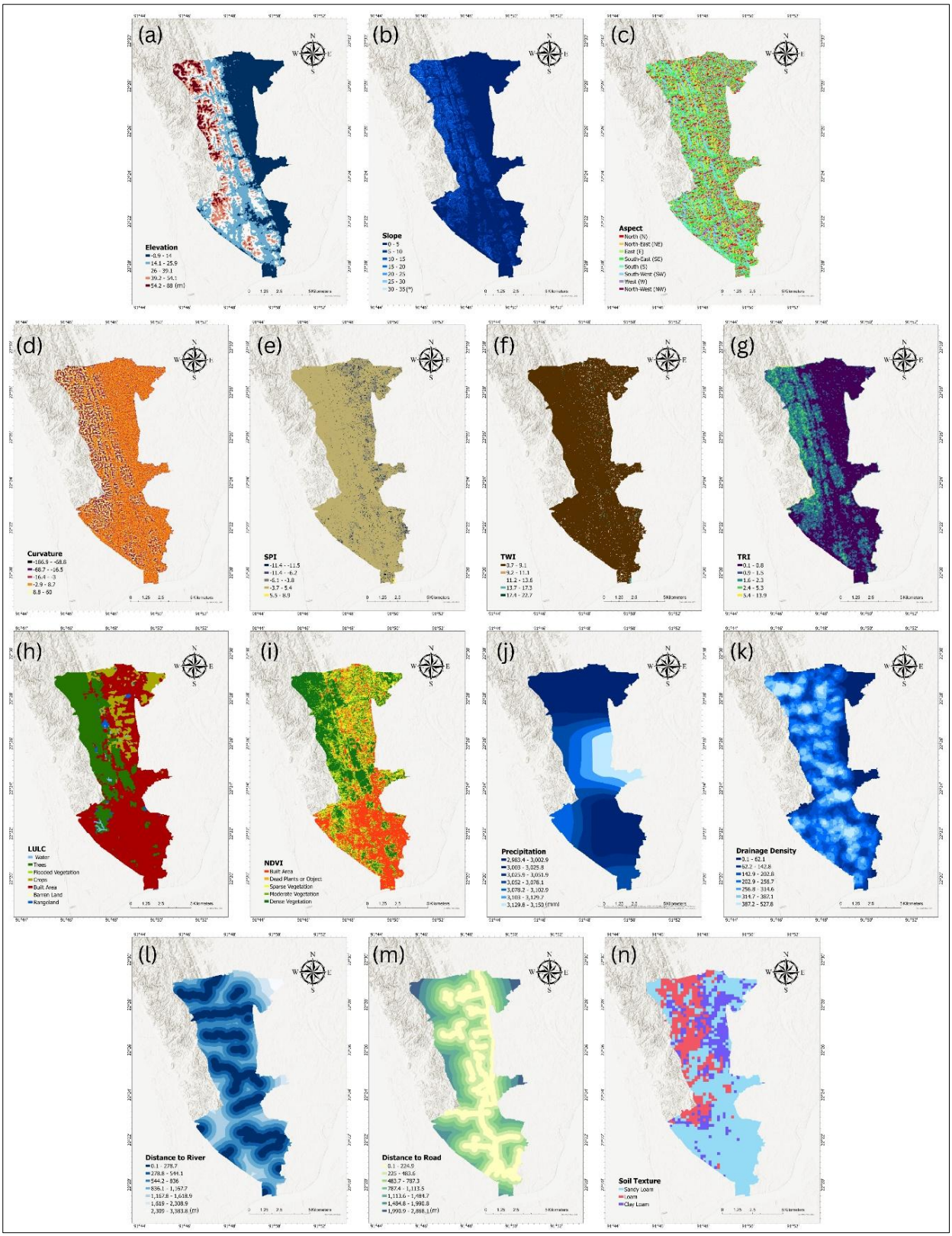

Figure 2: (a)Elevation, (b)Slope, (c)Aspect, (d)Curvature, ISPI, (f)TWI, (g)TRI, (h)LULC, (i)NDVI, (j)Precipitation, (k)Drainage Density, (l)Distance to River, (m)Distance to Road, (n)Soil Texture.

Methodology

This study presents an integrated Bayesian machine-learning framework for landslide susceptibility mapping (LSM), which incorporates flexibility-revealed preposing, probabilistic modeling, multilevel testing, and uncertainty-aware spatial deployment. The workflow begins with the compilation of historical landslide records and the associated conditioning factors, followed by standard preprocessing operations. Multivariate analysis, assessment, imputation, and feature scaling were conducted only on the training data set (Nair, 2024) beginning with an exploratory data analysis (EDA). All steps were performed carefully to prevent data leakage. Both classes of models (Bayesian: Bayesian Logistic Regression, Gaussian Process Classifier; conventional benchmark) are trained in the same pipeline configurations for a fair comparison. The proposed model performance is evaluated using a comprehensive validation strategy, along with repeated stratified cross-validation, spatial block cross-validation to assess the geographic generalization of results, and an independent holdout test for external evaluation (Shojaeezadeh et al., 2024). Discrimination, calibration, and probabilistic error metrics are jointly analyzed, and formal statistical tests are applied to identify groups that differ significantly. Final model selection is also based on performance assessments within a weighted multi-criteria rank-based framework that balances predictive power, spatial stability, and calibration fit. The chosen Bayesian model was then retrained on the entire dataset to produce a bivariate map of landslide susceptibility and uncertainty.

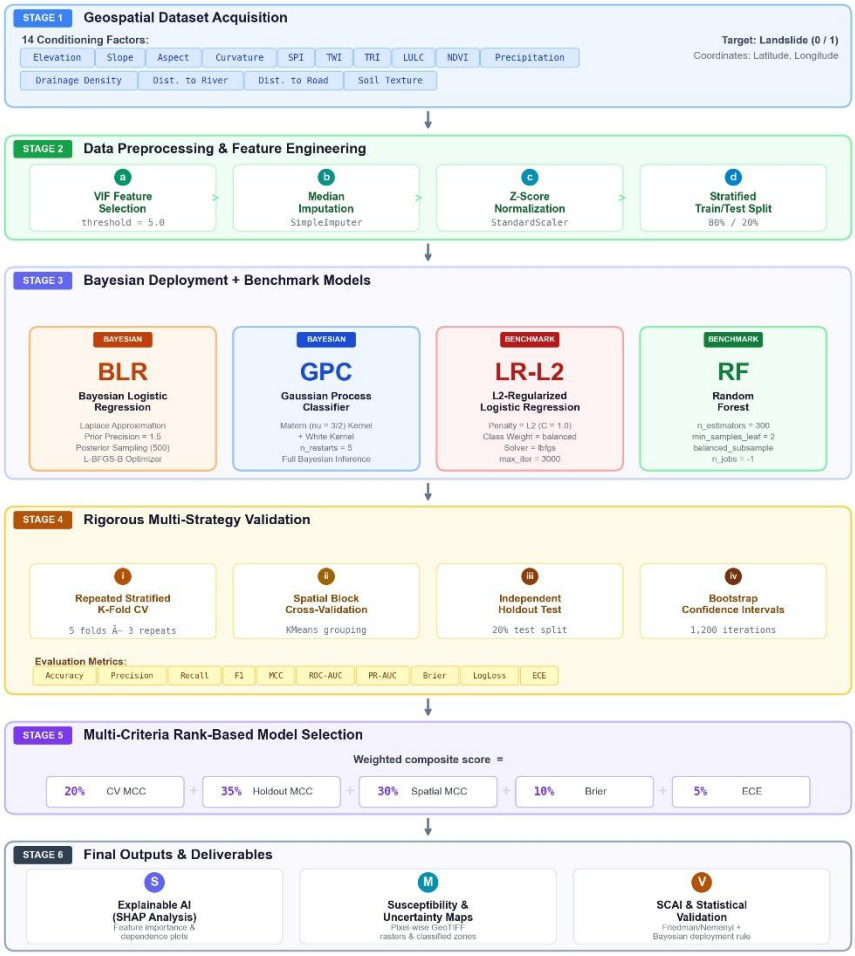

Figure 3: Methodological workflow for Bayesian deployment with benchmark comparison.

Multicollinearity screening

We evaluated multicollinearity among the conditioning factors prior to model development to ensure that regression-based and kernel-based models would be statistically stable and interpretable (Bobb et al., 2018). Predictor intercorrelation induces inflation in variance estimates, destabilizes coefficient estimation, and distorts posterior uncertainty of inference based on Bayesian frameworks (Gregorich et al., 2021). Hence, the multicollinearity diagnostics were carried out only on the training subset to avoid any information leakage into the validation stages (Truong et al., 2025).

In this study, multicollinearity was assessed using the Variance Inflation Factor (VIF) and its reciprocal, the Tolerance (TOL) index. For each predictor variable X_j, a regression model was fitted against all remaining predictors, and the corresponding coefficient of determination R_j^2 was computed. The tolerance value is defined as:

$$\text{Tolerance}_j = 1 - R_j^2 \qquad (1)$$

The Variance Inflation Factor is then calculated as:

$$\text{VIF}_j = \frac{1}{\text{Tolerance}_j} \qquad (2)$$

where R_j^2 represents the coefficient of determination obtained when the j^{th} The predictor is regressed on the remaining predictors.

Following established recommendations in susceptibility modeling studies, predictors with VIF values greater than 5 were considered indicative of substantial multicollinearity and were iteratively removed. The iterative elimination process continued until all remaining predictors met the predefined VIF criterion (Manczinger et al., 2025).

Machine Learning Models

Four classification algorithms were implemented within a unified preprocessing and validation framework to ensure methodological consistency, while conventional models were included as discriminative benchmarks. These algorithms were selected based on various studies in the literature (Bhatti et al., 2024).

Bayesian Logistic Regression (BLR)

Bayesian Logistic Regression was implemented as a probabilistic linear classifier using a logit link function (Genkin et al., 2007). Regression coefficients were treated as random variables with zero-mean Gaussian priors (Zucknick & Richardson, 2014), and the intercept remained unpenalized (Ghosal et al., 2025). The Laplace method was used for posterior inference, employing a multivariate normal approximation centered around the maximum a posteriori estimate (Sisti et al., 2024). Probability predictions were obtained by marginalizing the posterior distribution of model parameters, enabling direct quantification of predictive uncertainty via propagation of posterior variance (Cheng et al., 2022; Ting, 2025). The BLR model was chosen for its interpretability, regularization under moderate sample sizes, and use in probabilistic landslide susceptibility modelling (Das et al., 2012).

Gaussian Process Classifier (GPC)

The Gaussian Process Classifier was used as a non-parametric Bayesian model that can learn non-linear relationships between conditioning factors and landslide occurrence (Lisart-Liebermann & Medina, 2025; Zhang & YUE, 2024). A Gaussian Process prior with a Matérn covariance kernel was defined that provides an adequate trade-off between flexibility and smoothness to model spatially structured processes in the environment (Booth & Carpin, 2023; North et al., 2023). Due to the non-Gaussian nature of the likelihood, posterior inference was approximated via the Laplace method (Lombardo et al., 2018). The GPC not only produces predictive probabilities, but also latent variance estimates, allowing explicit characterization of epistemic uncertainty and more complicated decision boundaries in comparison to linear models (Ting, 2025).

L2-Regularized Logistic Regression (LR-L2)

We used a simple linear benchmark, L2-regularized Logistic Regression. Ridge regularization was applied to constrain coefficients, combat overfitting, and enhance generalizability (Şensoy et al., 2020). We addressed class imbalance through balanced class weighting. Unlike its Bayesian counterpart, LR-L2 provides point parameter estimates without posterior uncertainty, and we included it to evaluate the added value of Bayesian inference in terms of calibration and spatial robustness (Black et al., 2022).

Random Forest (RF)

Random Forest was implemented as an ensemble tree-based classifier using bootstrap aggregation and random feature selection. The model captures non-linear interactions without parametric assumptions (Pope et al., 2024). A balanced subsampling strategy was adopted to address class imbalance. Although RF typically demonstrates strong discriminative performance in landslide susceptibility studies, it does not provide coherent posterior uncertainty; therefore, it was treated strictly as a benchmark model in this research (Lv et al., 2025).

Validation design

To obtain statistically robust and spatially realistic performance estimates, three complementary validation strategies were implemented. First, repeated stratified cross-validation (5-fold × 3 repeats) was applied to the training subset to generate stable average metrics while preserving class proportions within each fold (Porrello et al., 2019). Second, we employed stratified sampling to reserve 20% of the data as an independent holdout set untouched by model development and reserved solely for external evaluation. Third, we performed spatial block cross-validation using GroupKFold and spatial clusters derived from KMeans clustering in geographic coordinates (Nothdurft et al., 2025). This approach maintains spatial separation between training and test samples, approximating spatial independence and curbing metric inflation resulting from spatial autocorrelation (Singh et al., 2025).

Evaluation metrics

A wide range of discrimination, robustness, and probabilistic calibration metrics were used for model evaluation to ensure balanced and statistically meaningful assessment of landslide susceptibility predictions. Both threshold-dependent and threshold-independent measures were considered (Halder et al., 2025). Metrics based on confusion matrices summarize concordance in class predictions at a fixed decision threshold, whereas ranking-based metrics characterize the model's ability to distinguish between landslide and non-landslide locations irrespective of threshold selection (Tehrani et al., 2022). As the suggested framework primarily centers on

probabilistic forecasting, especially for Bayesian models, we integrated proper scoring rules to evaluate the goodness of predicted probabilities, not just class labels (Mwakapesa et al., 2024). Additionally, calibration metrics were added to consider the reliability between predicted susceptibility probabilities and observed landslide occurrence (Pareek et al., 2024). This integrated evaluation approach guarantees a simultaneous assessment of discrimination strength, class-imbalance robustness, probability accuracy, and calibration reliability before model selection and spatial deployment.

$$\text{Accuracy} = \frac{TP + TN}{TP + TN + FP + FN} \quad (3)$$

$$\text{Precision} = \frac{TP}{TP + FP} \quad (4)$$

$$\text{Recall} = \frac{TP}{TP + FN} \quad (5)$$

$$\text{F1} = 2 \cdot \frac{\text{Precision} \cdot \text{Recall}}{\text{Precision} + \text{Recall}} \quad (6)$$

$$\text{MCC} = \frac{TP \cdot TN - FP \cdot FN}{\sqrt{(TP + FP)(TP + FN)(TN + FP)(TN + FN)}} \quad (7)$$

$$\text{TPR} = \frac{TP}{TP + FN} \quad (8)$$

$$\text{FPR} = \frac{FP}{FP + TN} \quad (9)$$

$$\text{Brier} = \frac{1}{n}\sum_{i=1}^{n}(p_i - y_i)^2 \quad (10)$$

$$\text{LogLoss} = -\frac{1}{n}\sum_{i=1}^{n}[y_i \log(p_i) + (1 - y_i)\log(1 - p_i)] \quad (11)$$

$$ECE = \sum_{k=1}^{K}\frac{n_k}{n}|acc(B_k) - conf(B_k)| \quad (12)$$

Where:
TP, TN, FP, FNdenote true positives, true negatives, false positives, and false negatives; $p_i$is the predicted probability for observation i; $y_i \in \{0,1\}$is the observed label;$n$is the total number of samples; $B_k$denotes the k^{th}probability bin; $n_k$is the number of samples in bin k; acc$(B_k)$is empirical accuracy within the bin k; conf$(B_k)$is the mean predicted probability in the bin k.

This formulation of metrics provides a clear and reproducible way to evaluate and is consistent with both traditional classification semantics and uncertainty-based probabilistic modeling goals.

Model Comparison, Selection, and Spatial Deployment Framework

To evaluate if differences in predictive performance were statistically significant, nonparametric hypothesis testing was performed on repeated cross-validation F1 scores (Mwakapesa et al., 2024). Since several models were assessed in the same folds, differences in global performance across groups were assessed using the Friedman test (Y. Yan et al., 2018). Significance was confirmed using the Friedman test ($\alpha = 0.05$) prior to performing pairwise

comparisons to determine specific model differences with the Nemenyi post-hoc test (Gardner & Brooks, 2018).

Following the statistical comparison, final model selection was performed using a weighted rank-based multi-criteria framework that integrates discrimination performance, spatial robustness, and probabilistic calibration. Each model was ranked across five criteria: (i) cross-validation MCC (20%), (ii) holdout MCC (35%), (iii) spatial block MCC (30%), (iv) holdout Brier score (10%, lower is better), and (v) holdout Expected Calibration Error (5%, lower is better) (Khan et al., 2025). The composite score was computed as a weighted average of normalized ranks; deployment was restricted to Bayesian candidates (Bayesian Logistic Regression and Gaussian Process Classifier) to ensure consistency between the susceptibility-mapping and uncertainty-representation objectives (Torizin et al., 2024).

In order to promote decision-oriented interpretation, susceptibility and predictive uncertainty were jointly visualized using a bivariate classification scheme (Kangas et al., 2023). Quantile thresholds were applied to obtain three ordinal classes (low, moderate, and high) for continuous susceptibility probabilities as well as normalized predictive variance class variables that preserved balanced spatial representation. The resulting 3×3 matrix was used to combine these classes into nine composite categories representing all combinations of susceptibility–uncertainty (Ghasemian et al., 2022). In this way, it permits the concurrent identification of high-susceptibility regions, confirmed by low infrastructural estimates (high susceptibility–low uncertainty), midzones with mixed characteristics (moderate combinations), and spatially uncertain predictions associated with significant indeterminacy. The bivariate representation enhances transparency by clearly demarcating confidently identified hazard hotspots from those where elevated susceptibility co-occurs with reduced certainty in the model's predictions (Agrawal & Dixit, 2023).

To evaluate the spatial concentration effectiveness of susceptibility classes, the Seed Cell Area Index (SCAI) was computed for each tier. SCAI quantifies the ratio between the spatial proportion of a susceptibility class and the proportion of landslides occurring within that class (Singh et al., 2024). Lower SCAI values in higher susceptibility tiers indicate improved concentration of landslides within smaller mapped areas, thereby reflecting more efficient hazard delineation (Zhao et al., 2023).

Results

Multicollinearity analysis

Multicollinearity diagnostics confirmed that all fourteen conditioning factors met the predefined thresholds (VIF < 5; TOL > 0.20). No predictors were excluded (Figure 4) in this dataset. VIF values ranged from 1.12 to 3.32, indicating low to moderate multicollinearity. Tolerance values (0.30–0.90) further confirmed the absence of critical redundancy in the data set. Overall, the predictor set was statistically stable and suitable for both Bayesian and benchmark modeling for landslide susceptibility mapping.

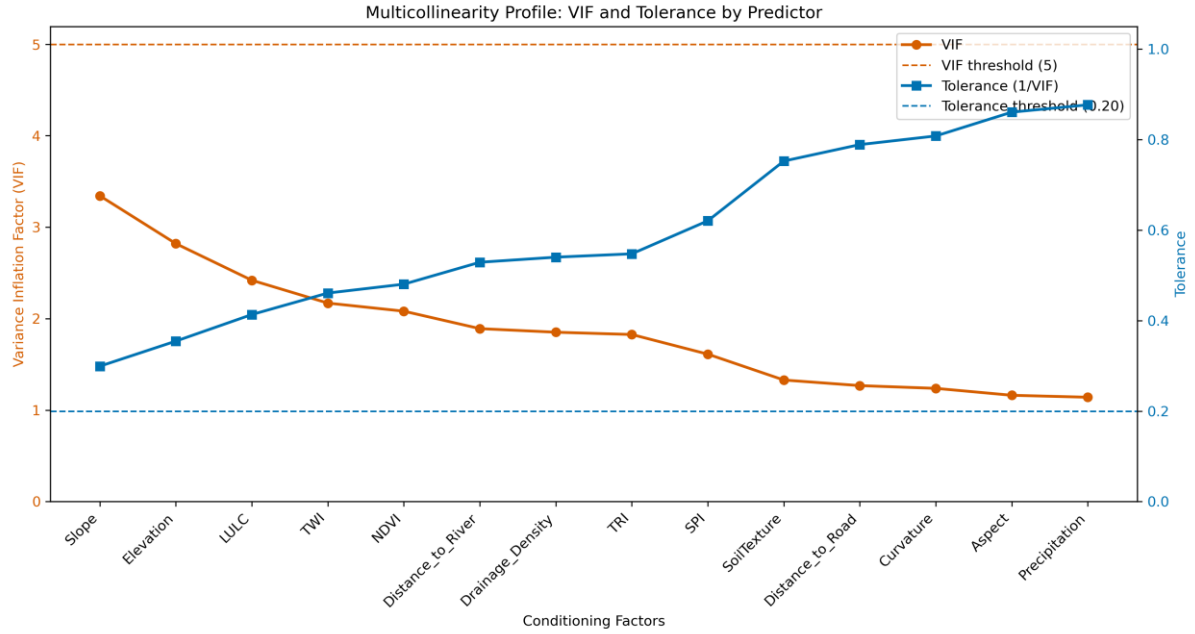

Figure 4: VIF and tolerance profile for the conditioning factors.

Holdout performance and multi-metric comparison

In the independent holdout evaluation (Table 2), Random Forest showed the strongest discrimination (ROC-AUC = 0.866; PR-AUC = 0.865) and overall agreement (MCC = 0.611). GPC (ROC-AUC = 0.821) achieved competitive discrimination among the Bayesian candidates and yielded the lowest calibration error overall (ECE = 0.084), indicating that GPC produced more reliable probabilities compared with BLR. Despite a high recall (0.774) reported by Bayesian logistic regression, lower precision and a higher Brier score indicated weaker probabilistic performance. Performance curves (Fig. 5) verify that RF prevails in the discrimination space. While RF had superior discriminative ability, GPC provided improved calibration stability, which is essential for probabilistic hazard communication.

Table 2: Holdout test performance (20% split).

Model	Accuracy	Precision	Recall	F1	MCC	ROC-AUC	PR-AUC	Brier	ECE
RF	0.811	0.774	0.774	0.774	0.611	0.866	0.865	0.153	0.120
GPC	0.743	0.676	0.742	0.708	0.481	0.821	0.814	0.172	0.084
LogReg_L2	0.703	0.615	0.774	0.686	0.420	0.768	0.667	0.203	0.110
BLR	0.676	0.606	0.645	0.625	0.340	0.775	0.723	0.193	0.112

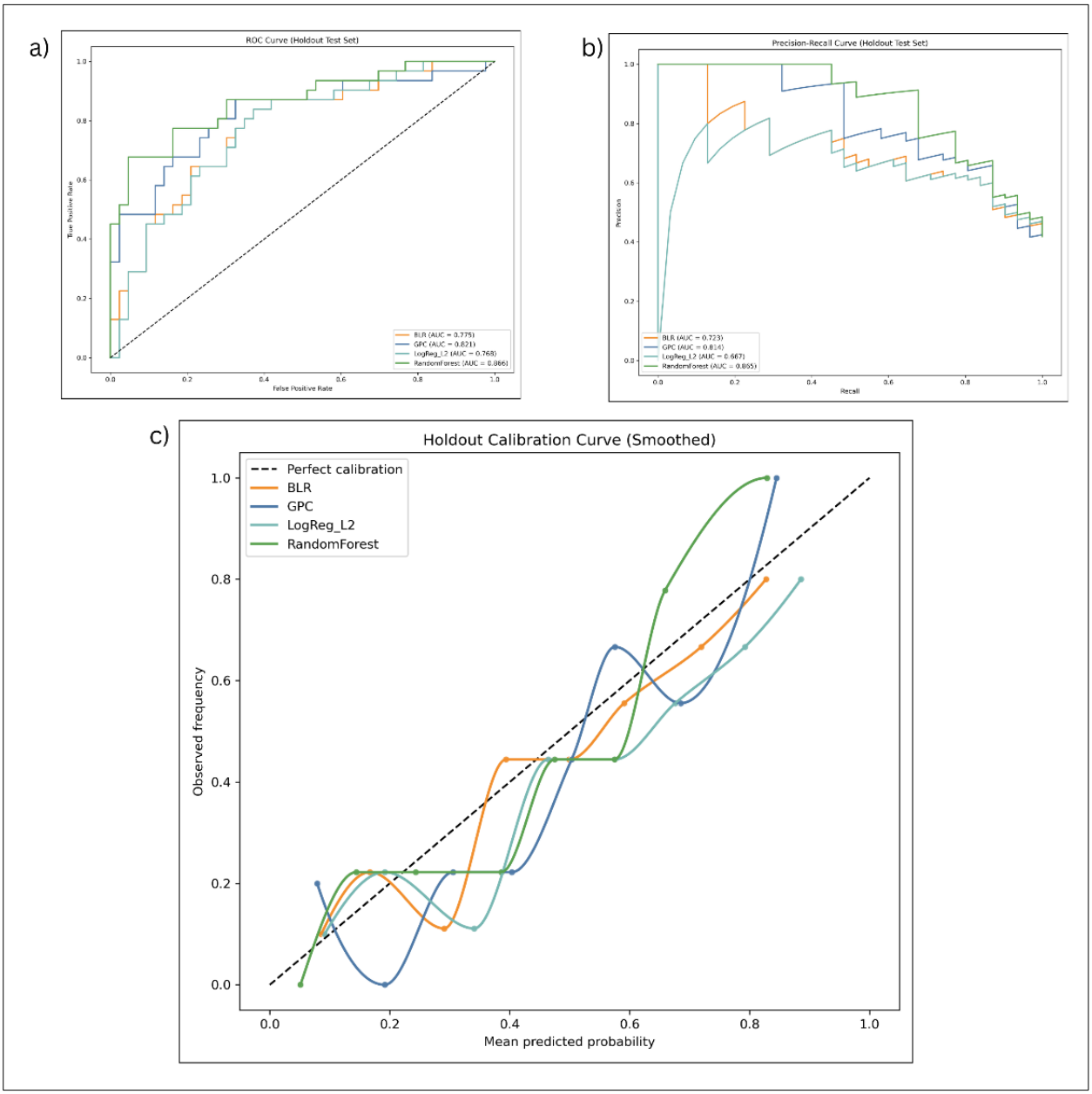

Figure 5: Holdout (test set) performance of all benchmarked models. ***(a)*** *ROC curves with AUC values.* ***(b)*** *Precision–Recall curves with PR-AUC values* ***(c)*** *Smoothed calibration curves; the dashed line indicates perfect calibration.*

Cross-validation and spatial generalization

Repeated stratified CV produced higher MCC and ROC-AUC values than spatial block CV (Table 3), indicating performance inflation under non-spatial validation. Spatial blocking reduced MCC by approximately 35% for RF (0.498 to 0.323) and 42% for GPC (0.450 to 0.259), highlighting the challenge of geographic transferability. Despite this degradation, model ranking remained stable, with RF and GPC consistently outperforming linear baselines under both validation schemes.

Table 3: Repeated CV and spatial block CV summary

Model	CV MCC (mean)	CV ROC-AUC (mean)	Spatial MCC (mean)	Spatial ROC-AUC (mean)
RF	0.498	0.849	0.323	0.805
GPC	0.450	0.836	0.259	0.769
LogReg_L2	0.433	0.756	0.214	0.709
BLR	0.388	0.757	0.226	0.709

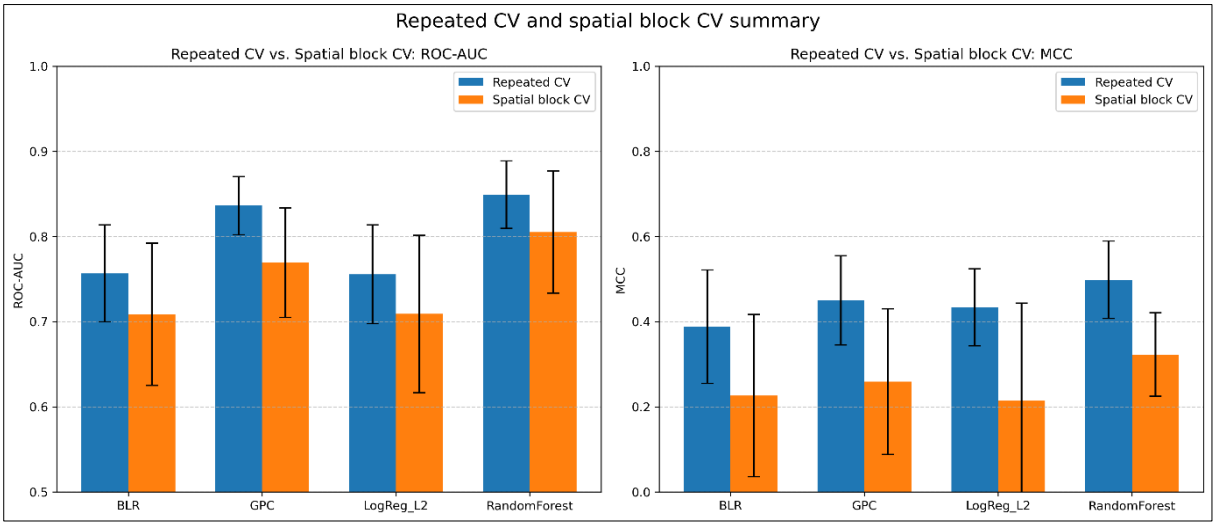

Figure 6: Comparison of repeated stratified CV and spatial block CV performance (MCC and ROC-AUC) across models.

Statistical significance and model ranking

The Friedman test on repeated cross-validation F1 scores showed significant differences between models ($\chi^2 = 17.73$, $p < 0.001$). Weighted multi-metric ranking was performed next; Random Forest was ranked first, GPC, LogReg_L2, and BLR performed last. However, only Bayesian candidates were deployed because we needed to represent uncertainty explicitly, and RF scored the highest composite rank. Of these, GPC exhibited the highest overall calibration stability and spatial robustness and thus was chosen for final susceptibility and uncertainty mapping.

Interpretation of Conditioning Factor Contributions

SHAP analysis (Fig. 7a) identified Elevation, Precipitation, and LULC as the most dominant predictors. Increased gravitational stress and slope-gradient effects at higher elevations positively contribute to SHAP, while the positive contributions of high precipitation values result from hydrological destabilization mechanisms through reduced pore-water pressure. The effect of LULC was found to be class-specific, which suggests the dependency of slope stability on vegetation coverage and human disturbance. The waterfall plot (Fig. 7b) shows that combined feature interactions propel predictions from the baseline of the model to a high-susceptibility local outcome scale.

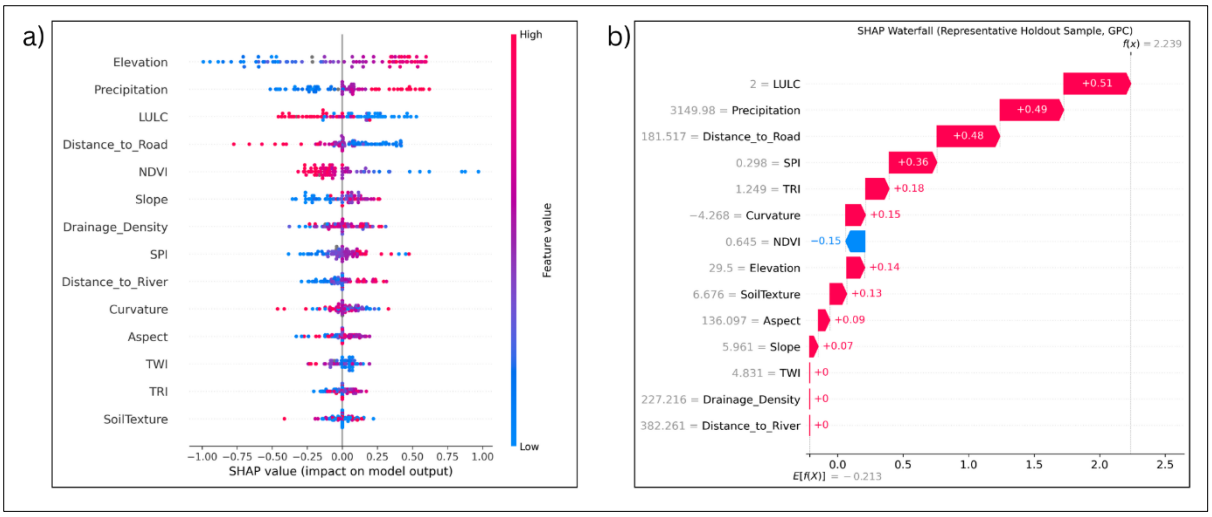

Figure 7: Interpretation of the GPC via SHAP on holdout dataset (a) SHAP summary (beeswarm) plot of the aggregated contribution and direction of influence of each conditioning factor to model predictions. (b) SHAP waterfall plot for a representative holdout sample showing the cumulative contribution of individual features from expected value $E[f(X)]$to the final predicted output $f(x)$.

Integrated Susceptibility–Uncertainty Patterns

Figure 8 illustrates a 3×3 bivariate classification of susceptibility and predictive uncertainty jointly conditioned on the output of the deployed GPC model. This modeling facilitates joint evaluation of forecasted hazard strength and model certainty in a spatial context.

Areas of high susceptibility are mostly clustered along the central and southeastern hill sectors of the study area, exhibiting well-defined clusters in space that track steep terrain and anthropogenically disturbed slopes. A significant fraction of these zones falls into classes with uncertainty on the low- or medium-side of the scale, implying that the local density of training data supports stable posterior predictions. Regions like these are potential landslide hotspots, with high confidence.

On the other hand, localized patches exhibit high susceptibility and high uncertainty. These zones primarily develop in border terrain and vadose zones and peripheral hill zones. Areas for which the predicted probability and variance were both high are indicative of lower posterior stability, perhaps due to heterogeneous geomorphological conditions or a training inventory that is not representative in those areas. Data in these areas should be interpreted with caution and potentially could benefit from localized field-based validation.

Low-susceptibility areas predominate in the northeastern and relatively flat sectors of the study area. These areas are typically regions of low predictive uncertainty providing confidence in mapped stable terrain. Nonetheless, neighborhoods of moderate uncertainty on low-

susceptibility classes reveal model sensitivity near the susceptibility threshold for isolated sectors.

Overall, the bivariate analysis shows that most high-susceptibility clusters are underpinned by relatively low uncertainty, providing greater confidence in hazard delineation while transparently highlighting areas where predictive certainty is lessened.

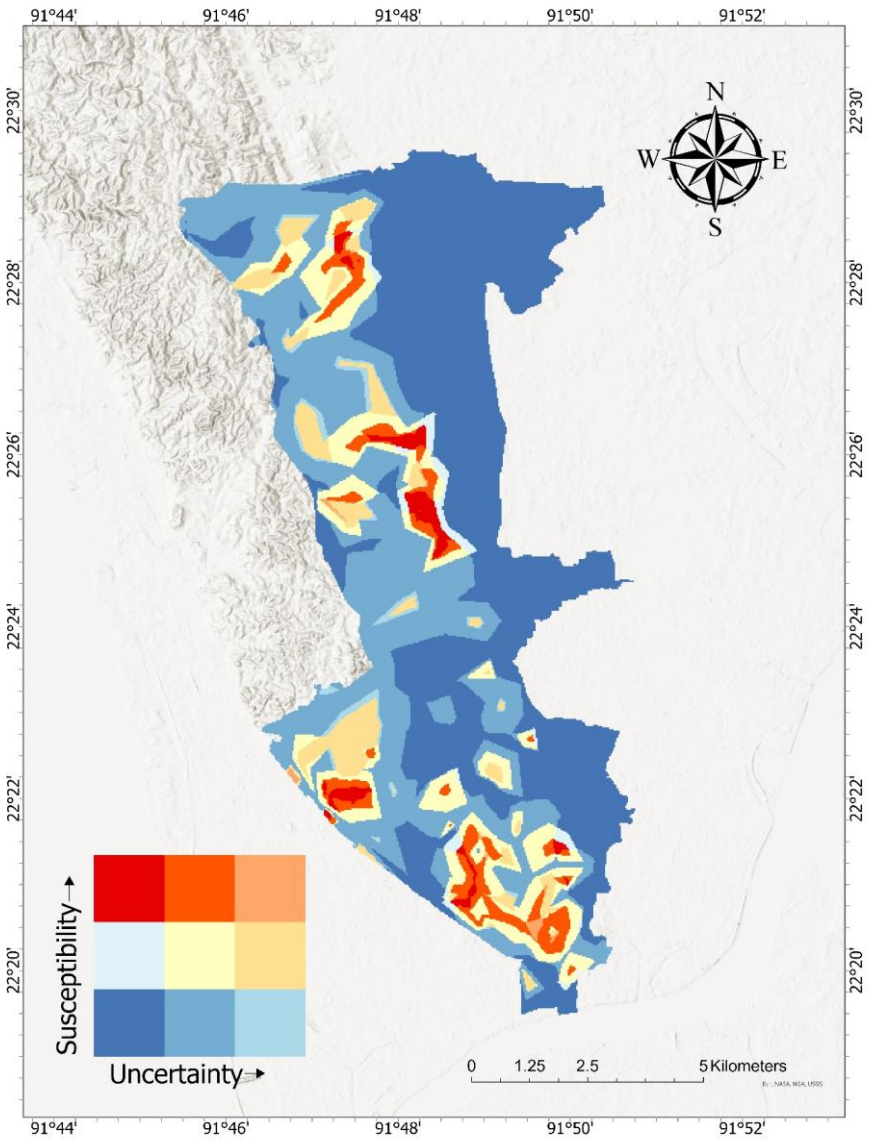

Figure 8: *Bivariate landslide susceptibility–uncertainty map based on deployed Gaussian Process Classifier. Susceptibility (vertical axis) and predictive uncertainty (horizontal axis) were categorized into three ordinal classes based on quantile thresholds and combined into a 3 × 3 matrix. The color of the squares indicates the combined classification of susceptibility and predictive uncertainty.*

Susceptibility stratification is robust according to SCAI analysis (please see Table 4). More specifically, the Very High class was predictive because it contains 78.71% of all mapped landslides but covers only 9.47% of the study area. On the other hand, the Very Low and Low classes, which together cover over 50% of the area, account for only 1.3% of the landslides. The significant decrease in SCAI from Very Low (45.53) to Very High (0.12) represents good spatial discrimination as well as the significance of hazard zonation.

Table 4 SCAI by susceptibility tier.

Tier	Area %	Landslide %	Landslide Count	SCAI
Very Low	29.37	0.65	1	45.53
Low	23.16	0.65	1	35.90
Moderate	24.04	5.81	9	4.14
High	13.96	14.19	22	0.98
Very High	9.47	78.71	122	0.12

Discussion

The comparative evaluation of deterministic and Bayesian classifiers reveals the trade-off between discriminative strength and probabilistic reliability. Random Forest showed the best discrimination on our independent holdout dataset, confirming its ability to model nonlinear interactions between geomorphological and hydrological predictors. Earlier studies have also shown that RF is effective for landslide susceptibility mapping (Halder et al., 2025; Naceur et al., 2026). However, calibration analysis provides a more sophisticated reading. Though the Random Forest achieved the highest scores on the ROC-AUC and MCC metrics, the Gaussian Process Classifier (GPC) exhibited the lowest Expected Calibration Error, indicating the best agreement between predicted probabilities and observed landslide frequency. Hence, the multi-criteria framework with weights focuses on achieving balanced performance across discrimination, calibration, and spatial robustness to select which one to deploy from GPC. Its selection in the current study was additionally justified by its improved predictive performance and lower false-positive rates compared with other models, resulting in a more reliable and robust evaluation of landslide susceptibility (Singh et al., 2025).

The explicit comparison between repeated stratified cross-validation and spatial block cross-validation highlights the necessity of geographically realistic validation schemes (Wang et al., 2023). Performance under spatial blocking corroborates that random cross-validation overestimates metrics due to spatial autocorrelation effects in training and testing samples (Wang et al., 2023). However, differences between models persisted across test schemes, indicating stable model behavior. Bayesian models can further reduce overconfidence by representing the uncertainty in extrapolated regions (Ting, 2025). The increased predictive variance at the transition zones of susceptibility indicates either insufficient local training support or lower posterior certainty.

The bivariate susceptibility–uncertainty representation refines hazard interpretation by differentiating between robust and uncertain hotspots. In central hill sectors, high susceptibility coincides with low posterior variance, indicating strong model support. Peripheral hill margins exhibit elevated susceptibility with higher uncertainty, suggesting extrapolation beyond well-represented conditions. The Seed Cell Area Index (SCAI) results validate the spatial concentration efficiency of the final model. The Very High susceptibility class contains nearly four-fifths of mapped landslides while occupying less than one-tenth of the study area, indicating strong stratification. The monotonic decline in SCAI values confirms the effectiveness of hazard zonation.

Interpretability analysis based on SHAP values provides geomorphological plausibility. Elevation, precipitation, and land use/land cover emerged as dominant predictors. The consistency of feature importance across validation schemes indicates alignment with established physical understanding.

Despite its methodological rigor, the study has limitations. The landslide inventory remains modest in size, and additional temporal records could enhance posterior stability. Rainfall was incorporated as a climatological layer rather than event-based intensity, limiting temporal sensitivity (Moreno et al., 2023). Spatial interpolation may smooth localized micro-topographic effects. Future research may incorporate event-scale rainfall thresholds, hierarchical spatial priors, or hybrid physics–Bayesian neural network frameworks (Yan et al., 2025).

Conclusion

This study develops and evaluates an uncertainty-aware landslide-susceptibility framework using Bayesian and deterministic classifiers with a unified preprocessing and validation strategy for Chattogram's hilly area. The findings show how evaluation metrics alone can overestimate predictive capability when accounting for spatial autocorrelation. Overall, although Random Forest delivered the best discrimination performance, its predictive capability was hindered by inadequate probabilistic calibration and uncertainty estimation, unlike the Gaussian Process Classifier. However, GPC provided nearly comparable predictions and improved performance by offering well-calibrated uncertainty estimates, which are vital for risk-informed decision-making.

With the Bayesian model deployed, we modeled continuous surfaces of susceptibility and predictive variance, then combined them via bivariate classification to separate robust hazard hotspots from spatially uncertain predictions. Hazard stratification was also supported by spatial concentration analyses, with most historical landslides concentrated in a small fraction of the mapped area and some clustered within that area.

This study integrates discrimination assessment, spatial cross-validation, calibration analysis, statistical comparison, and uncertainty visuals into a workflow, advancing landslide susceptibility modeling toward a transparent, decision-oriented framework. This is especially suited for fast-urbanizing, data-poor hill terrains where hazard prioritization considers both probability and confidence. Concepts like an area of applicability could further improve transparency by indicating where predictions are reliable.

References

Adnan, M. S. G., Rahman, M. S., Ahmed, N., Ahmed, B., Rabbi, M. F., & Rahman, R. M. (2020). Improving Spatial Agreement in Machine Learning-Based Landslide Susceptibility Mapping. *Remote Sensing*, *12*(20), 3347–3347. https://doi.org/10.3390/rs12203347

Agrawal, N., & Dixit, J. (2023). GIS-based landslide susceptibility mapping of the Meghalaya-Shillong Plateau region using machine learning algorithms. *Bulletin of Engineering Geology and the Environment*, *82*(5). https://doi.org/10.1007/s10064-023-03188-2

Ahmed, B. (2014). Landslide susceptibility mapping using multi-criteria evaluation techniques in Chittagong Metropolitan Area, Bangladesh. *Landslides*, *12*(6), 1077–1095. https://doi.org/10.1007/s10346-014-0521-x

Bhatti, A., Angkan, P., Behinaein, B., Mahmud, Z., Rodenburg, D., Braund, H., Mclellan, P. J., Ruberto, A. J., Harrison, G. L. A., Wilson, D. G., Szulewski, A., Howes, D., Etemad, A., & Hungler, P. (2024). CLARE: Cognitive Load Assessment in REaltime with Multimodal Data. *arXiv (Cornell University)*. https://doi.org/10.48550/arxiv.2404.17098

Biswas, N., Islam, K. M. A., Efty, E. A., Das, S., Pathan, A. M., & Ferdaus, M. R. (2026). Ensemble deep learning framework for landslide susceptibility mapping and road vulnerability index development in the Chittagong Hill Tracts, Bangladesh. *Geomatics Natural Hazards and Risk*, *17*(1). https://doi.org/10.1080/19475705.2026.2634207

Black, B., Strien, M. J. van, Adde, A., & Grêt-Regamey, A. (2022). Re-considering the status quo: Improving calibration of land use change models through validation of transition potential predictions. *Environmental Modelling & Software*, *159*, 105574–105574. https://doi.org/10.1016/j.envsoft.2022.105574

Bobb, J. F., Henn, B. C., Valeri, L., & Coull, B. A. (2018). Statistical software for analyzing the health effects of multiple concurrent exposures via Bayesian kernel machine regression. *Environmental Health*, *17*(1). https://doi.org/10.1186/s12940-018-0413-y

Booth, L., & Carpin, S. (2023). Informative path planning for scalar dynamic reconstruction using coregionalized Gaussian processes and a spatiotemporal kernel. *arXiv (Cornell University)*. https://doi.org/10.48550/arxiv.2309.07340

Cheng, C. H., & Fan, L. (2024). Uncertainty of interpretability in Landslide Susceptibility Mapping: A Comparative Analysis of Statistical, Machine Learning, and Deep Learning Models. *arXiv (Cornell University)*. https://doi.org/10.48550/arxiv.2405.11762

Cheng, L., Yin, F., Theodoridis, S., Chatzis, S., & Chang, T.-H. (2022). Rethinking Bayesian Learning for Data Analysis: The art of prior and inference in sparsity-aware modeling. *IEEE Signal Processing Magazine*, *39*(6), 18–52. https://doi.org/10.1109/msp.2022.3198201

Chowdhury, M. S., Rahman, M. N., Sheikh, M. S., Sayeid, M. A., Mahmud, K. H., & Hafsa, B. (2023). GIS-based landslide susceptibility mapping using logistic regression, random forest and decision and regression tree models in Chattogram District, Bangladesh. *Heliyon*, *10*(1). https://doi.org/10.1016/j.heliyon.2023.e23424

Cunha, R. L. F., Silva, B., & Netto, M. A. S. (2018). *A Scalable Machine Learning System for Pre-Season Agriculture Yield Forecast*. 423–430. https://doi.org/10.1109/escience.2018.00131

Das, I., Stein, A., Kerle, N., & Dadhwal, V. K. (2012). Landslide susceptibility mapping along road corridors in the Indian Himalayas using Bayesian logistic regression models. *Geomorphology*, *179*, 116–125. https://doi.org/10.1016/j.geomorph.2012.08.004

Ehsan, M. M., Anees, M. T., Bakar, A. F. A., & Ahmed, A. (2025, September). A review of geological and triggering factors influencing landslide susceptibility: Artificial intelligence-based trends in mapping and prediction. In *International Journal of Environmental Science and Technology*. Springer Science+Business Media. https://doi.org/10.1007/s13762-025-06741-6

Gardner, J., & Brooks, C. (2018). Dropout Model Evaluation in MOOCs. *Proceedings of the AAAI Conference on Artificial Intelligence*, *32*(1). https://doi.org/10.1609/aaai.v32i1.11392

Genkin, A., Lewis, D., & Madigan, D. (2007). Large-Scale Bayesian Logistic Regression for Text Categorization. *Technometrics*, *49*(3), 291–304. https://doi.org/10.1198/004017007000000245

Ghasemian, B., Shahabi, H., Shirzadi, A., Al-Ansari, N., Jaafari, A., Kress, V. R., Geertsema, M., Renoud, S., & Ahmad, A. (2022). A Robust Deep-Learning Model for Landslide Susceptibility Mapping: A Case Study of Kurdistan Province, Iran. *Sensors*, *22*(4), 1573–1573. https://doi.org/10.3390/s22041573

Ghosal, P., De, S., & Ghosh, J. (2025). An Online Algorithm for Bayesian Variable Selection in Logistic Regression Models With Streaming Data. *arXiv (Cornell University)*. https://doi.org/10.48550/arxiv.2501.10930

Gregorich, M., Strohmaier, S., Dunkler, D., & Heinze, G. (2021). Regression with Highly Correlated Predictors: Variable Omission Is Not the Solution. *International Journal of Environmental Research and Public Health*, *18*(8), 4259–4259. https://doi.org/10.3390/ijerph18084259

Hafsa, B., Chowdhury, M. S., & Rahman, M. N. (2022). Landslide susceptibility mapping of Rangamati District of Bangladesh using statistical and machine intelligence model. *Arabian Journal of Geosciences*, *15*(15). https://doi.org/10.1007/s12517-022-10607-3

Halder, K., Srivastava, A. K., Ghosh, A., Das, S., Banerjee, S., Pal, S. C., Chatterjee, U., Bisai, D., Ewert, F., & Gaiser, T. (2025). Improving landslide susceptibility prediction through ensemble recursive feature elimination and meta-learning framework. *Scientific Reports*, *15*(1). https://doi.org/10.1038/s41598-025-87587-3

Hamza, A., Talha, M., Shah, A. H., Khokhar, S. A., Khan, M. H., Khushnood, R. A., & Ahmed, T. (2025). Advanced structural interventions for slope stabilization and disaster resilience. *Discover Geoscience*, *3*(1). https://doi.org/10.1007/s44288-025-00199-2

Hengl, T., Jesus, J. M. de, Heuvelink, G. B. M., González, M. R., Kilibarda, M., Blagotić, A., Shangguan, W., Wright, M. N., Geng, X., Bauer-Marschallinger, B., Guevara, M., Vargas, R., MacMillan, R. A., Batjes, N. H., Leenaars, J. G. B., Ribeiro, E., Wheeler, I., Mantel, S., & Kempen, B. (2017). SoilGrids250m: Global gridded soil information based on machine learning. *PLoS ONE*, *12*(2). https://doi.org/10.1371/journal.pone.0169748

Hen-Jones, R., Zapata, C., Jiménez, E., Holcombe, E., & Vardanega, P. J. (2025). Community-scale slope stability assessment of urbanisation scenarios in North Quito, Ecuador. *Landslides*. https://doi.org/10.1007/s10346-025-02608-6

Islam, M. A., Islam, M. S., & Jeet, A. A. (2021). A Geotechnical Investigation of 2017 Chattogram Landslides. *Geosciences*, *11*(8), 337–337. https://doi.org/10.3390/geosciences11080337

Kangas, A., Myllymäki, M., & Mehtätalo, L. (2023). Understanding uncertainty in forest resources maps. *Silva Fennica*. https://doi.org/10.14214/sf.22026

Khan, R. A., BAREERA, Shah, A., VEGA -MURILLO, & Khan, H. U. (2025). Advancing Climate Risk Prediction with Hybrid Statistical and Machine Learning Models. *Research Square (Research Square)*. https://doi.org/10.21203/rs.3.rs-7477242/v1

Koldasbayeva, D., Tregubova, P., Gasanov, M., Zaytsev, A., Petrovskaia, A., & Burnaev, E. (2024, December). Challenges in data-driven geospatial modeling for environmental research and practice. In *Nature Communications* (Vol. 15, Issue 1, pp. 10700–10700). Nature Portfolio. https://doi.org/10.1038/s41467-024-55240-8

Lisart-Liebermann, T., & Medina, A. C. (2025). Preconditioning Natural and Second Order Gradient Descent in Quantum Optimization: A Performance Benchmark. *arXiv (Cornell University)*. https://doi.org/10.48550/arxiv.2504.16518

Lombardo, L., Opitz, T., & Huser, R. (2018). Point process-based modeling of multiple debris flow landslides using INLA: an application to the 2009 Messina disaster. *Stochastic Environmental Research and Risk Assessment*, *32*(7), 2179–2198. https://doi.org/10.1007/s00477-018-1518-0

Lv, M., Li, K., Cai, J., Jun, M., Gao, J., & Xu, H. (2025). Evaluation of landslide susceptibility based on SMOTE-Tomek sampling and machine learning algorithm. *PLoS ONE*, *20*(5). https://doi.org/10.1371/journal.pone.0323487

Manczinger, M., Kovács, L., & Kovács, T. (2025). Fire susceptibility assessment in the Carpathians using an interpretable framework. *Scientific Reports*, *15*(1). https://doi.org/10.1038/s41598-025-10296-4

Milà, C., Ludwig, M., Pebesma, E., Tonne, C., & Meyer, H. (2024). Random forests with spatial proxies for environmental modelling: Opportunities and pitfalls. *Geoscientific Model Development*, *17*(15), 6007–6033. https://doi.org/10.5194/gmd-17-6007-2024

Mirus, B. B., & Woodard, J. (2023). *Bayesian logistic regression and optimized XGBoost models for landslide susceptibility assessment*. https://doi.org/10.5194/egusphere-egu23-11586

Moreno, M., Lombardo, L., Crespi, A., Zellner, P., Mair, V., Pittore, M., Westen, C. J. van, & Steger, S. (2023). Space-time data-driven modeling of precipitation-induced shallow landslides in South Tyrol, Italy. *EarthArXiv (California Digital Library)*. https://doi.org/10.31223/x59m3j

Mwakapesa, D. S., Lan, X., & Mao, Y. (2024). Landslide susceptibility assessment using deep learning considering unbalanced samples distribution. *Heliyon*, *10*(9). https://doi.org/10.1016/j.heliyon.2024.e30107

Naceur, H. A., Igmoullan, B., Namous, M., Lassiane, Y., Benazun, H., Mallick, J., Hang, H. T., & Abdo, H. G. (2026). Integrating geospatial data and hybrid machine learning

models for landslide susceptibility assessment in semi-arid environments. *Geomatics Natural Hazards and Risk*, *17*(1). https://doi.org/10.1080/19475705.2026.2625403

Nair, A. (2024). Geospatial Analysis of Landslide Susceptibility Through Machine Learning In Relation to Environmental Indicators Across Global Regions. *EarthArXiv (California Digital Library)*. https://doi.org/10.31223/x5471f

North, J. S., Risser, M. D., & Breidt, F. J. (2023). A flexible class of priors for orthonormal matrices with basis function-specific structure. *arXiv (Cornell University)*. https://doi.org/10.48550/arxiv.2307.13627

Nothdurft, A., Sarkleti, V., Ofner-Graff, T., Tockner, A., Gollob, C., Ritter, T., Kraßnitzer, R., Svazek, P., Kühmaier, M., Stampfer, K., & Finley, A. O. (2025). Small area estimation of growing stock timber volume, basal area, mean stem diameter, and stem density for mountain forests in Austria. *arXiv (Cornell University)*. https://doi.org/10.48550/arxiv.2506.05043

Pareek, T., Bhuyan, K., Westen, C. J. van, Rajaneesh, A., Sajinkumar, K. S., & Lombardo, L. (2024). Analyzing the posterior predictive capability and usability of landslide susceptibility maps: A case of Kerala, India. *Landslides*, *22*(3), 655–670. https://doi.org/10.1007/s10346-024-02389-4

Poddar, I., & Roy, R. (2026). Assessing landslide susceptibility mapping in the Sikkim Himalayas using an ensemble machine learning approach. *Discover Geoscience*, *4*(1). https://doi.org/10.1007/s44288-025-00375-4

Pope, F. D., Baruah, A., Bousiotis, D., Damayanti, S., Bigi, A., Ghermandi, G., Ghaffarpasand, O., & Harrison, R. M. (2024). A novel spatiotemporal prediction approach to fill air pollution data gaps using mobile sensors, machine learning and citizen science techniques. *Research Square (Research Square)*. https://doi.org/10.21203/rs.3.rs-4667713/v1

Porrello, A., Vincenzi, S., Buzzega, P., Calderara, S., Conte, A., Ippoliti, C., Candeloro, L., Lorenzo, A. D., & Dondona, A. C. (2019). *Spotting Insects from Satellites: Modeling the Presence of Culicoides Imicola Through Deep CNNs*. 159–166. https://doi.org/10.1109/sitis.2019.00036

Rabby, Y. W., & Li, Y. (2019). Landslide Inventory (2001–2017) of Chittagong Hilly Areas, Bangladesh. *Data*, *5*(1), 4–4. https://doi.org/10.3390/data5010004

Rahman, M. M., Joy, M. F. R., Ahmed, A., Tabassum, A., Sarker, M. S., & Barman, T. K. (2025). Comparative multi-criteria decision-making approaches for landslide susceptibility mapping in Khagrachhari district of southeastern Bangladesh. *Research Square (Research Square)*. https://doi.org/10.21203/rs.3.rs-7362869/v1

Roy, S. K., Zidan, M. Z. R., Ullah, M. S., & Moniruzzaman, M. (2025). Landslide susceptibility assessment in Chittagong division using remote sensing, GIS, and machine learning. *Discover Geoscience*, *3*(1). https://doi.org/10.1007/s44288-025-00337-w

Şensoy, M., Kaplan, L., Cerutti, F., & Saleki, M. (2020). Uncertainty-Aware Deep Classifiers Using Generative Models. *Proceedings of the AAAI Conference on Artificial Intelligence*, *34*(4), 5620–5627. https://doi.org/10.1609/aaai.v34i04.6015

Shaker, M., & Hüllermeier, E. (2025). Random forest calibration. *Knowledge-Based Systems*, *328*, 114143–114143. https://doi.org/10.1016/j.knosys.2025.114143

Shojaeezadeh, S. A., Elnashar, A., & Weber, T. K. D. (2024). A Novel Fusion of Optical and Radar Satellite Data for Crop Phenology Estimation using Machine Learning and Cloud Computing. *arXiv (Cornell University)*. https://doi.org/10.48550/arxiv.2409.00020

SINDHU, S. (2025). *Stacking Ensemble Learning: Combining XGBoost, LightGBM, CatBoost, and AdaBoost with Random Forest Meta Model*. https://doi.org/10.21203/rs.3.rs-7944070/v1

Singh, A., Dhiman, N., Niraj, K. C., & Shukla, D. P. (2024). "Ensembled transfer learning approach for error reduction in landslide susceptibility mapping of the data scare region." *Scientific Reports*, *14*(1). https://doi.org/10.1038/s41598-024-76541-4

Singh, G., Rosman, B., Byrne, M. J., & Reynolds, C. (2025). An earth observation and explainable machine learning approach for determining the drivers of invasive species—A water hyacinth case study. *Environmental Monitoring and Assessment*, *197*(11). https://doi.org/10.1007/s10661-025-14517-1

Sisti, A. J., Zullo, A. R., & Gutman, R. (2024). A Bayesian Method for Adverse Effects Estimation in Observational Studies with Truncation by Death. *arXiv (Cornell University)*. https://doi.org/10.48550/arxiv.2410.04561

Song, Y., Guo, J., Ma, F., Liu, J., & Li, G. (2023). Spatial distribution analysis and application of engineering disturbance disasters in the Himalayan alpine valley. *Frontiers in Earth Science*, *10*. https://doi.org/10.3389/feart.2022.1098631

Stefanini, F. M., Ambrosini, S., & D′Alessandro, F. (2025). vulneraR: An R Package for Uncertainty Analysis in Coastal Vulnerability Studies. *Mathematics*, *13*(22), 3603–3603. https://doi.org/10.3390/math13223603

Sun, D., Wen, H., Xu, J., Zhang, Y., Wang, D., & Zhang, J. (2021). Improving Geospatial Agreement by Hybrid Optimization in Logistic Regression-Based Landslide Susceptibility Modelling. *Frontiers in Earth Science*, *9*. https://doi.org/10.3389/feart.2021.713803

Tai, X., Anderegg, W. R. L., Blanken, P. D., Burns, S. P., Christensen, L., & Brooks, P. D. (2020). Hillslope Hydrology Influences the Spatial and Temporal Patterns of Remotely Sensed Ecosystem Productivity. *Water Resources Research*, *56*(11). https://doi.org/10.1029/2020wr027630

Tehrani, F. S., Calvello, M., Liu, Z., Zhang, L., & Lacasse, S. (2022). Machine learning and landslide studies: Recent advances and applications. *Natural Hazards*, *114*(2), 1197–1245. https://doi.org/10.1007/s11069-022-05423-7

Ting, Y.-S. (2025). Statistical Machine Learning for Astronomy – A Textbook. *arXiv (Cornell University)*. https://doi.org/10.48550/arxiv.2506.12230

Torizin, J., Fuchs, M., Balzer, D., Kuhn, D., Glaser, S., Ehret, D., Wiedenmann, J., Dommaschk, P., Henscheid, S., & Strauß, R. (2024). Project '"Mass Movements in Germany"' and its implications for nationwide landslide susceptibility assessment. *Bulletin of Engineering Geology and the Environment*, *83*(6). https://doi.org/10.1007/s10064-024-03691-0

Truong, O., Zhang, T., Marchareddy, A., Lee, S.-B., Busold, J., Socas, M., & AlOmar, E. A. (2025). LeakageDetector 2.0: Analyzing Data Leakage in Jupyter-Driven Machine Learning Pipelines. *arXiv (Cornell University)*. https://doi.org/10.48550/arxiv.2509.15971

Tsompanakis, Y., Makrakis, N., Psarropoulos, P. N., & Frangopol, D. M. (2023). Climate change impact on the integrity of structures and infrastructure in mountainous or hilly areas. In *CRC Press eBooks* (pp. 515–522). Informa. https://doi.org/10.1201/9781003323020-61

Tulbure, M. G., Broich, M., Perin, V., Gaines, M. D., Ju, J., Stehman, S. V., Pavelsky, T., Masek, J. G., Yin, S., Mai, J., & Betbeder-Matibet, L. (2022). Can we detect more ephemeral floods with higher density harmonized Landsat Sentinel 2 data compared to Landsat 8 alone? *Carolina Digital Repository (University of North Carolina at Chapel Hill)*. https://doi.org/10.17615/nx7d-ra05

Wang, Y., Khodadadzadeh, M., & Zurita-Milla, R. (2023). Spatial+: A new cross-validation method to evaluate geospatial machine learning models. *International Journal of Applied Earth Observation and Geoinformation*, *121*, 103364–103364. https://doi.org/10.1016/j.jag.2023.103364

Xia, L., Shen, J., Zhang, T., Dang, G., & Wang, T. (2023). GIS-based landslide susceptibility modeling using data mining techniques. *Frontiers in Earth Science*, *11*. https://doi.org/10.3389/feart.2023.1187384

Yan, W.-J., Mei, L.-F., Yin, Y.-H., Mo, J., Papadimitriou, C., Yuen, K.-V., & Beer, M. (2025, May). Bayesian Learning in Structural Dynamics: A Comprehensive Review and Emerging Trends. In *arXiv (Cornell University)*. Cornell University. https://doi.org/10.48550/arxiv.2505.22223

Yan, Y., Yin, X.-C., Yang, C., Li, S., & Zhang, B. (2018). Biomedical literature classification with a CNNs-based hybrid learning network. *PLoS ONE*, *13*(7). https://doi.org/10.1371/journal.pone.0197933

Zhang, X., & YUE, J. (2024). Predictive Modeling of Student Performance Through Classification with Gaussian Process Models. *International Journal of Advanced Computer Science and Applications*, *15*(6). https://doi.org/10.14569/ijacsa.2024.01506123

Zhao, R., Ameri, A., & santosh, M. (2023). Land subsidence susceptibility mapping: A new approach to improve Decision Stump Classification (DSC) performance and combine it with four machine learning algorithms. *Research Square (Research Square)*. https://doi.org/10.21203/rs.3.rs-2747324/v1

Zhou, X., & Xing, Y. (2025). Spatial consistency assessment and landslide susceptibility prediction optimization. *Frontiers in Earth Science*, *13*. https://doi.org/10.3389/feart.2025.1702688

Zucknick, M., & Richardson, S. (2014). MCMC algorithms for Bayesian variable selection in the logistic\textbackslashn regression model for large-scale genomic applications. *arXiv (Cornell University)*. https://doi.org/10.48550/arxiv.1402.2713